Journal of Chemical&Engineering Data

pubs.acs.org/jced

Article

Effects of Different Oxygen-Containing Co-solvents' Molecular Structure and Intermolecular Forces on the Solubility of Methanol-Renewable Diesel Fuel Blends

Huaying Wang-Alho,* Fatimoh Balogun,* Katriina Sirviö, Carolin Nuortila, David Thomas, Maciej Mikulski, and Seppo Niemi

Cite This: *J. Chem. Eng. Data* 2026, 71, 2901−2913

Read Online

ACCESS | Metrics & More | Article Recommendations | Supporting Information

ABSTRACT: The limited solubility of methanol in diesel fuels necessitates the use of co-solvents to achieve homogeneous and stable blends. This study investigated the effectiveness of two higher alcohols (1-octanol and 1-dodecanol) and one short-chain ester (methyl butyrate) in improving the miscibility of methanol with a renewable diesel. Methanol-renewable diesel blends with methanol energy shares ranging from 5% to 90% were prepared, and co-solvents were titrated until a clear single-phase mixture was obtained. Ternary phase diagrams were used to characterize the phase behavior at room temperature. Intermolecular interactions governing blend stability were analyzed using Hansen solubility parameters, complemented by ATR-FTIR spectroscopy to assess changes in hydrogen bonding and molecular polarity. The results demonstrate that the co-solvent molecular structure strongly influences blending performance. Higher alcohols exhibited superior effectiveness compared to the ester, with 1-dodecanol providing the highest stabilization efficiency, followed by 1-octanol, while methyl butyrate showed the poorest performance. The enhanced performance of higher alcohols is attributed to their ability to balance dispersion forces and hydrogen-bonding interactions, as supported by Hansen solubility parameter analysis. These findings offer mechanistic insight into methanol-renewable diesel miscibility and provide practical guidance for co-solvent selection in methanol-based compression-ignition fuel formulations.

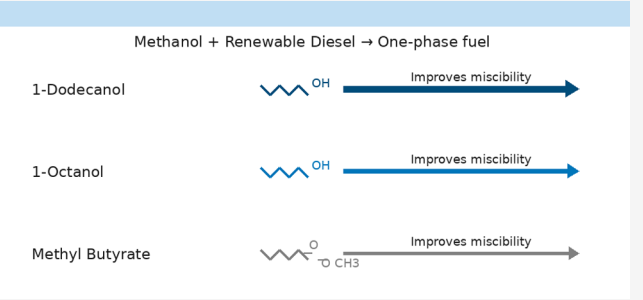

1. INTRODUCTION

Energy from fossil fuels has been the driving force behind social development since the Industrial Revolution.[1] However, combustion of fossil fuels significantly contributes to environmental pollution,[2,3] and it is necessary to reduce greenhouse gas (GHG) emissions. Coupled with the increasing demand for energy and the price volatility of crude oil, this has led to concerted efforts to research and develop alternative energy sources.[4] Much of the vehicle sector can be electrified,[5] but internal combustion engines are considered necessary to achieve sufficient power output and range[6] in sectors such as maritime, nonroad vehicles, and heavy on-road transportation.[6] The need to mitigate the environmental impacts of these applications creates a need for research on renewable fuels.[6−8]

The International Maritime Organization (IMO) has set the target to reduce annual greenhouse gas emissions from international shipping to net zero by or around 2050.[9] Achieving this reduction calls for coordinated research in both engine technologies and low-carbon fuel formulations to find cleaner, renewable fuels to maximize power-system efficiency with the lowest possible emissions.

Methanol, particularly when produced from renewable sources, is considered a promising alternative low-carbon fuel for decarbonizing maritime engines.[10] It can be produced entirely from renewable sources via thermochemical routes or biochemical pathways.[11] Future methanol production can use renewable hydrogen and captured carbon dioxide (CO_2).[12] Methanol exhibits desirable characteristics for combustion, such as a high stoichiometric fuel-to-air ratio, high oxygen content, high hydrogen-to-carbon ratio, and a significant latent heat of evaporation, enabling a wide engine-load range. This contributes to the reduction of nitrogen oxides (NOx) emissions and soot.[13,14] However, these properties necessitate a highly reactive fuel to facilitate controlled self-ignition in low-temperature combustion (LTC) conditions. Renewable diesel is considered one of the most reactive renewable alternatives for facilitating clean combustion because its chemical structure exhibits favorable autoignition properties. It is a good option to reduce

Received: March 1, 2026
Revised: May 5, 2026
Accepted: June 4, 2026
Published: June 17, 2026

https://doi.org/10.1021/acs.jced.6c00133
J. Chem. Eng. Data 2026, 71, 2901−2913

the marine sector's climate impact and can be made from renewable raw materials such as used cooking oil, animal fat from food industry waste, or crude tall oil, a residue of pulp production. Renewable diesel's life-cycle GHG emissions are lower than those of fossil diesel's, and good quality renewable diesel is compatible with all compression ignition (CI) engines.[15−17] Renewable diesel's paraffinic structure also mitigates the formation of particulate matter.[15,18]

Combining methanol and renewable diesel is a promising way to utilize their combustion properties as efficiently as possible while producing low emissions. Ammar[19] demonstrated that the use of methanol-diesel dual-fuel engines can substantially reduce exhaust emissions, achieving reductions of 77% for NOx, 89% for sulfur oxides (SOx), 55% for carbon monoxide (CO), 18% for CO_2, and 83% for particulate matter (PM). Emulsification can address methanol's lubricity issues when blending methanol and renewable diesel prior to injection. Furthermore, when mixing methanol and renewable diesel, the fuel blend does not result in a stable single-phase mixed fuel.[20] Therefore, achieving stable single-phase methanol-renewable diesel blends prior to injection facilitates reliable fuel handling and engine operation.

Co-solvents, such as furans, alcohols, ethers, and esters,[21] act as bridging agents through molecular compatibility and bonding to produce a homogeneous and stable single-phase blend.[22] Co-solvents significantly influence the solubility characteristics of fuel blends, but their effectiveness depends on their molecular structure, such as alkyl carbon chain length and oxygen-containing functional groups.[23] Oxygenates, such as alcohols, are generally polar compounds, whereas hydrocarbon fuels are nonpolar,[24] thus causing the miscibility problem when blending alcohol and diesel fuels. Increasing the content of oxygen-containing additives in the blend helps to reduce smoke emissions.[25−27]

Methanol (MeOH, CH_3OH), a simple alcohol, consists of a hydroxyl group (−OH) attached to a methyl group ($-CH_3$). This structure facilitates hydrogen bonding, a significant intermolecular force, and imparts high polarity to the molecule.[28] However, the hydroxyl group also causes methanol to phase separate in hydrocarbons.[29] Methanol's hydrogen-bonding capability enhances its solubility in water and other polar solvents.[30,31] Conversely, renewable diesel comprises long-chain saturated hydrocarbons (C_{15}−C_{18}), which are nonpolar paraffinic components.[32,33] Renewable diesel's molecular structure primarily exhibits weak van der Waals forces (dispersion forces) as its primary intermolecular interaction, resulting in poor solubility in polar solvents like methanol.[32] It is well-established that polar molecules dissolve in polar solvents, and nonpolar molecules dissolve in nonpolar solvents, adhering to the principle of "like dissolves like".[28] The intermolecular forces significantly influence the solubility of substances. The co-solvents 1-octanol, 1-dodecanol, and methyl butyrate exhibit varying degrees of hydrogen bonding, dipole−dipole interactions, and dispersion forces,[23] which influence their ability to bridge the polarity gap between methanol and renewable diesel.

In the study by Li et al.,[34] long-chain alcohol co-solvents were found to enhance the miscibility of ethanol/diesel blends. The energy analysis indicated that the hydrogen bonding and van der Waals interactions were the main driving forces to improve miscibility, while the polarization interaction made no major contribution. Hydrogen bonding was predominant for short-chain alcohols, whereas van der Waals interactions were crucial for long-chain alcohols. The coordination of hydrogen bonding and van der Waals energy in dynamic equilibrium led to optimal miscibility.[34] Both alcohols 1-octanol ($C_8H_{17}OH$) and 1-dodecanol ($C_{12}H_{25}OH$) possess hydroxyl groups that facilitate hydrogen bonding (−OH), contributing to their solubility in polar solvents.[28] Additionally, their long alkyl chains promote hydrophobic interactions, enhancing solubility with nonpolar substances. Methyl butyrate ($C_5H_{10}O_2$) is an ester characterized by a short alkyl chain. Its molecular structure features a methyl group (CH_3-) attached to butyric acid through an ester bond, which includes the polar carboxylate functional group.[28] Unlike alcohols, esters lack hydroxyl groups, meaning that methyl butyrate cannot form hydrogen bonds through the hydroxyl functionality.

Wang-Alho et al.[20] investigated 1-dodecanol, 1-octanol, and methyl butyrate as oxygenated co-solvents to form a stable mixture of methanol and renewable diesel. Otherwise, research on the blending properties of renewable diesel and methanol with different co-solvents is scarce, and it is important to understand the chemical interactions occurring between the components when evaluating their properties as a fuel blend.

The Hansen solubility parameters (HSPs) characterize the solubility of the various binary and ternary systems.[35] HSPs are based on the principle that the total energy of vaporization of a liquid can be divided into three components: a dispersion force part, a permanent dipole-permanent dipole force part, and a hydrogen-bonding part. Materials with similar HSPs exhibit high affinity for each other. A stable solution needs a similar distribution of intermolecular forces among solvent−solvent, solvent−solute, and solute−solute interactions.[23] Therefore, by treating methanol as a solute, it is feasible to dissolve methanol in renewable diesel by adjusting the HSPs of the diesel/co-solvent mixture.

In addition to HSP analysis, spectroscopic techniques are essential for elucidating molecular-level interactions. Balogun et al. evaluated the feasibility of Fourier transform infrared (FTIR) analytics for determining the stability of methanol-renewable diesel mixtures.[36] They discussed FTIR spectroscopy as a powerful tool to analyze the molecular interactions between methanol, renewable diesel, and co-solvents (1-dodecanol, 1-octanol, and methyl butyrate) in blended fuels. FTIR spectroscopy and molecular dynamics simulation methods can be combined to provide fundamental understanding of solubility behavior, phase stability, and molecular interactions, thus helping to understand the miscibility mechanism at a molecular level.[36]

Against this background, advancing non-fossil maritime fuel options requires understanding the mechanisms governing the solubility of a fully renewable methanol-renewable diesel blend. This research analyzed the molecular structure and intermolecular forces of three co-solvents in methanol-renewable diesel solutions: 1-dodecanol, 1-octanol, and methyl butyrate. The effect of co-solvents on methanol-fossil diesel solubility is already known: this study aims to fill the knowledge gap concerning their solubility effect specifically for renewable diesel with methanol. The methanol blending shares in the experimental work were raised from 5% to 90%, and co-solvents were gradually added until a clear and homogeneous phase was achieved. The Hansen solubility parameters (HSPs) were used to quantify and characterize the intermolecular force contributions (dispersion, polar, and hydrogen bonding) in the methanol-renewable diesel-co-solvent systems. Ternary phase diagrams depict the phase behavior of the ternary system. In addition, FTIR analysis was used to detect and study changes in characteristic absorption bands associated with functional

https://doi.org/10.1021/acs.jced.6c00133
J. Chem. Eng. Data 2026, 71, 2901−2913

Table 1. Chemical Sample Table

chemical name	chemical formula	CAS number	supplier	initial purity	purification method	analytical method
methanol	CH_3OH	67-56-1	Merck KGaA/VWR	analysis grade	none	supplier certified analysis grade (purity verified by manufacturer)
renewable diesel (RD)	C15−C18 *n*-alkanes mixture	–	Neste, Finland	not reported	none	supplier certified commercial fuel product (quality verified according to EN 15940)
1-dodecanol	$C_{12}H_{26}O$	112-53-8	Merck KGaA/VWR	not reported	melted before use	supplier certified synthesis grade (purity verified by manufacturer)
1-octanol	$C_8H_{18}O$	111-87-5	Merck KGaA/VWR	99%	none	supplier certified synthesis grade (purity verified by manufacturer)
methyl butyrate	$C_5H_{10}O_2$	623-42-7	Thermo Fisher/VWR	99%	none	supplier certified laboratory chemical grade (purity verified by manufacturer)

Table 2. Physical and Chemical Properties of the Test Fuels and the Additives

	methanol[a]	renewable diesel[a]	1-dodecanol[b]	1-octanol[b]	methyl butyrate[b]
chemical formula	CH_3OH	C_nH_{2n+2}	$C_{12}H_{26}O$	$C_8H_{18}O$	$C_5H_{10}O_2$
oxygen content* (wt %)	49.9%	–	8.6%	12.3%	31.4%
density (kg/m^3) at 15 °C	795	782	820	830	897
lower heating value (MJ/kg)	20[37]	44[33]	–	37.6	–
kinematic viscosity (m^2/s) at 40 °C	0.55	3.14	–	5.60	–
boiling point (°C)	65	217	260	195	102
flash point (°C)	9	82	119	86	12

[a]Data adapted from Wang-Alho et al., 2023.[38] [b]Data from the manufacturer; −sign represents missing values; and * sign represents calculated results.

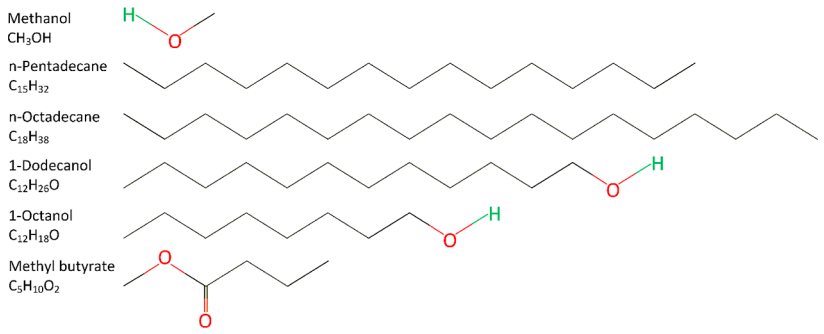

Figure 1. Chemical structures of methanol, renewable diesel (represented by *n*-alkanes C15−C18), 1-dodecanol, 1-octanol, and methyl butyrate.[39]

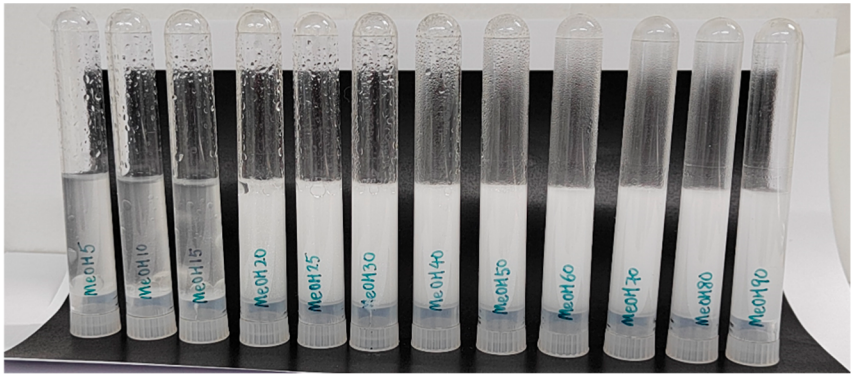

Figure 2. Blends of methanol and renewable diesel (from left to right) with methanol blend share of 5%, 10%, 15%, 20%, 25%, 30%, 40%, 50%, 60%, 70%, 80%, and 90%, respectively: blends are labeled MeOH5 to MeOH90 and were photographed immediately after preparation with the blends in one phase. The photograph was taken by one of the authors.

groups (i.e., O−H, C−H, C═O, and C−O), thereby revealing interactions such as hydrogen bonding or polarity shifts. As a result, the study evaluated how the molecular structure of each co-solvent enhances the solubility of methanol in renewable diesel.

2. MATERIALS AND METHODS

2.1. Materials

The research studied 12 methanol (MeOH)-renewable diesel (RD) blends. The methanol content in the blends varied from 5% to 90% (5%, 10%, 15%, 20%, 25%, 30%, 40%, 50%, 60%, 70%, 80%, and 90%,

https://doi.org/10.1021/acs.jced.6c00133
J. Chem. Eng. Data 2026, 71, 2901−2913

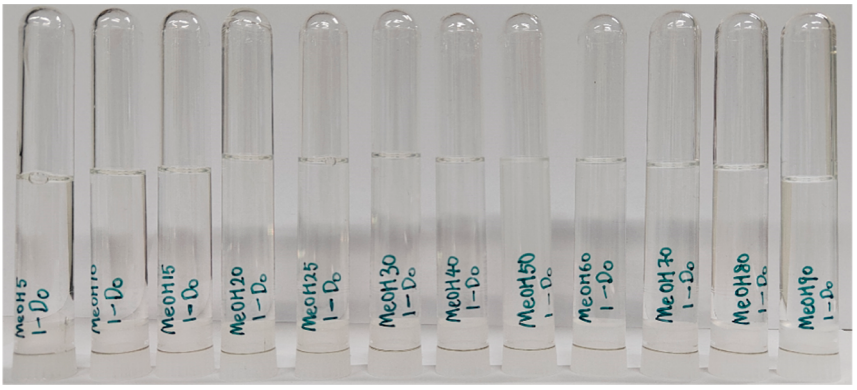

Figure 3. Stable single-phase methanol-renewable diesel blends with the co-solvent 1-dodecanol. The photograph was taken by one of the authors.

respectively). The blend shares were calculated on an energy basis prior to adding the co-solvents. The lower heating values used for calculations were 44 MJ kg^{-1} for renewable diesel[33] and 20 MJ kg^{-1} for methanol.[37] Methanol was Merck KGaA analysis grade and purchased from VWR, Finland. Renewable diesel was Neste Renewable Diesel supplied by Neste, Finland. The renewable diesel had no additives.

The three co-solvents, 1-dodecanol, 1-octanol, and methyl butyrate, were all purchased from VWR, Finland. The 1-dodecanol and 1-octanol were products of Merck KGaA; the methyl butyrate was a product of Thermo Fisher Scientific. The details of the chemical samples are summarized in Table 1. Table 2 lists the physical and chemical properties of the methanol and renewable diesel fuels and the three co-solvent additives.

Figure 1 presents the chemical structure depictions of methanol, renewable diesel, 1-dodecanol, 1-octanol, and methyl butyrate. Renewable diesel primarily consists of long-chain *n*-alkanes ranging from *n*-C_{15} to *n*-C_{18}, so the figure illustrates the molecular structures of *n*-pentadecane (C_{15}) and *n*-octadecane (C_{18}) as representative components. The chemical structures of *n*-hexadecane (C_{16}) and *n*-heptadecane (C_{17}) are analogous to those of C_{15} and C_{18}, respectively. Methanol (CH_3OH) contains a hydroxyl (−OH) functional group bonded to a single carbon atom. Both 1-dodecanol and 1-octanol are long-chain primary alcohols featuring terminal −OH groups attached to extended hydrocarbon chains. Methyl butyrate ($CH_3CH_2CH_2COOCH_3$) is an ester characterized by the presence of a carbonyl (C═O) group and C−O−C linkages within its molecular structure. In contrast, renewable diesel, composed predominantly of saturated hydrocarbons such as *n*-alkanes, lacks polar functional groups and consists mainly of C−H bonds within long chains.

2.2. Binary Methanol-Renewable Diesel Blends

Figure 2 shows 12 different proportions of methanol and renewable diesel fuel blends, ranging from 5% to 90% methanol. The samples are labeled from MeOH5 to MeOH90 according to their methanol content. Methanol and diesel begin to separate immediately when mixed, becoming completely phase-separated after about 2 h.

2.3. Titration Method to Measure the Needed Amount of Co-solvents for the Preparation of Ternary Blends

A titration method was used to assess how much of each co-solvent was needed to form a stable mixture of methanol and renewable diesel. The method followed that used by Gao et al.[23] A total of 12 fuel blends were evaluated, consisting of 5% of methanol and 95% of renewable diesel (MeOH5) to 90% of methanol and 10% of renewable diesel (MeOH90) (Figure 2). The co-solvent 1-dodecanol has a melting temperature range of 24−27 °C, so it was in a solid state at room temperature; it was melted in a warm water bath at approximately 30 °C to be handled.

The mixtures of methanol and renewable diesel were prepared in plastic tubes with an initial volume of 5 mL. Titration was performed at room temperature, with the co-solvent being added gradually to the mixture using a high-precision pipet with an accuracy of 0.1 μL. The titration endpoint was detected visually as the appearance of a clear, stable, one-phase liquid. The volume of the added co-solvent was recorded for this point. Test tubes with the fuel blends were mixed in a vortex mixer at 2400 rpm to prepare the blend solutions. Duplicates of each solution were prepared, and the final data presented here represents the average of the two independent titrations. The blends of methanol-renewable diesel and co-solvent were kept overnight and checked after 24 h to verify that they had remained stable. All three of the studied co-solvents were titrated in the same way. Figure 3 shows that mixed fuels with different proportions of methanol and renewable diesel formed stable single-phase fuels after adding 1-dodecanol.

2.3.1. Uncertainty Analysis. When determining the minimum amount of co-solvent required to form a clear and stable single-phase methanol-renewable diesel-*co*-solvent blend, the titration endpoint was identified visually as the formation of a homogeneous liquid phase. The uncertainty in the added co-solvent volume was governed by the accuracy of the high-precision pipet used during titration (±0.1 μL). The reported co-solvent contents correspond to the final minimum amount required to achieve phase stability, rather than a statistical ensemble of repeated endpoint measurements, so the uncertainty was estimated based on instrumental accuracy. The corresponding mass uncertainty was calculated as $\Delta m = \rho \cdot \Delta V$ and propagated to the co-solvent mass fraction as $\Delta w = \Delta m/\mathrm{m\_total}$. The resulting absolute uncertainty in co-solvent mass fraction is of the order of 10^{-5} (w/w), which is negligible relative to the observed differences in co-solvent demand among the studied systems. The Supporting Information provides complete ternary compositions and estimated uncertainties.

2.4. Solubility Parameters

The methanol in methanol-renewable diesel blends is highly polar, whereas the renewable diesel is nonpolar, leading to phase separation. Co-solvents bridge this polarity gap, and their effectiveness depends on molecular structure and intermolecular interactions. This study systematically rationalizes co-solvent selection by quantifying these interactions using solubility parameters. The Hildebrand solubility parameter (δ) is defined as the square root of the cohesive energy density (CED), which is the molar energy of vaporization divided by the molar volume of the liquid. One can predict the miscibility of different substances by comparing their Hildebrand solubility parameters. Substances with similar δ values are more likely to dissolve in each other and form a homogeneous solution, whereas significant differences in δ values indicate poor solubility.[23]

Hansen solubility parameters extend the Hildebrand solubility parameter by decomposing the total cohesive energy into three physically meaningful components. The correlation between the Hildebrand solubility parameter δ and HSPs conforms to eq 1.[1,40]

$$\delta^2 = \delta_d^2 + \delta_p^2 + \delta_h^2 \quad (1)$$

where δ_d is the dispersion solubility parameter, δ_p is the polar solubility parameter, and δ_h is the hydrogen-bonding solubility parameter.

The portion of HSPs contributing to the total solubility parameter can be determined using eqs 2−4.[40] In these equations, f denotes the

https://doi.org/10.1021/acs.jced.6c00133
J. Chem. Eng. Data 2026, 71, 2901−2913

fractional contribution of dispersion (f_d), polar (f_p), and hydrogen-bonding (f_h) interactions, respectively, reflecting the proportion of the total cohesive energy associated with each type of molecular interaction. Table 3 presents the Hansen solubility parameters of methanol, renewable diesel's components of hexadecane and octadecane, and the selected co-solvents, together with the fractional contributions of dispersion (f_d), polar (f_p), and hydrogen-bonding (f_h) interactions.[40] Table 3 shows a significant disparity in the solubility parameters between methanol and renewable diesel components. This highlights their immiscibility, which is considered in more detail in Section 4.

Table 3. Solubility Parameters of Studied Solvents and Fuels, According to Data from Gao et al. 2021[23]

reagents	δ	δ_d	δ_p	δ_H	f_d	f_p	f_h
methanol	29.7	15.1	12.3	22.3	0.30	0.25	0.45
1-octanol	20.56	16.0	5.0	11.9	0.49	0.15	0.36
1-dodecanol	18.93	16.0	4.0	9.3	0.54	0.14	0.32
methyl butyrate	17.71	–	–	–	–	–	–
renewable diesel components:							
hexadecane	16.3	16.3	0	0	1	0	0
octadecane[a]	16.4	16.4	0	0	1	0	0

[a]Data from Charles M. Hansen, 2007;[40]—unknown.

$$f_d = \frac{\delta_d}{\delta_d + \delta_p + \delta_h} \quad (2)$$

$$f_p = \frac{\delta_p}{\delta_d + \delta_p + \delta_h} \quad (3)$$

$$f_h = \frac{\delta_h}{\delta_d + \delta_p + \delta_h} \quad (4)$$

2.5. ATR-FTIR Spectroscopy

The attenuated total reflectance Fourier transform infrared (ATR-FTIR) spectroscopy was used for monitoring the chemical bond changes, quantitative analysis, and mixture characterization. Blends were prepared and stored at room temperature. After 4 weeks of storage, samples were scanned over the range of 4000−400 cm^{-1} with a resolution of 4 cm^{-1}. Analysis was undertaken with a Thermo Scientific Nicolet Summit X ATR-FTIR spectrometer, equipped with a diamond crystal measurement slab. The acquired spectra were subsequently processed and analyzed using Omnic Paradigm software (version 2.5). A more detailed description of this ATR-FTIR equipment as a methodology can be found in Balogun et al.[36]

All spectra were baseline-corrected and normalized to facilitate comparison. The normalized FTIR spectra are presented for neat methanol, binary methanol-renewable diesel blends, and ternary methanol-renewable diesel-co-solvent blends (Figures 7−10), and binary methanol-renewable diesel blends were mixed vigorously to form an emulsion. The FTIR spectrum was taken during temporary emulsion formation before separation occurred. FTIR spectra were measured for a total of 36 samples, each with different blend shares and different co-solvents. Samples were characterized using key FTIR spectral regions and absorption intensity to monitor changes in chemical bonds and shifts in molecular polarity.

3. RESULTS

Titration was used to determine the minimum volume of each co-solvent required to achieve a homogeneous methanol-renewable diesel mixture. All methanol-renewable diesel blended fuels were prepared with a total volume of 5 mL. Figure 4 shows the corresponding co-solvent volumes required to achieve stable single-phase blends.

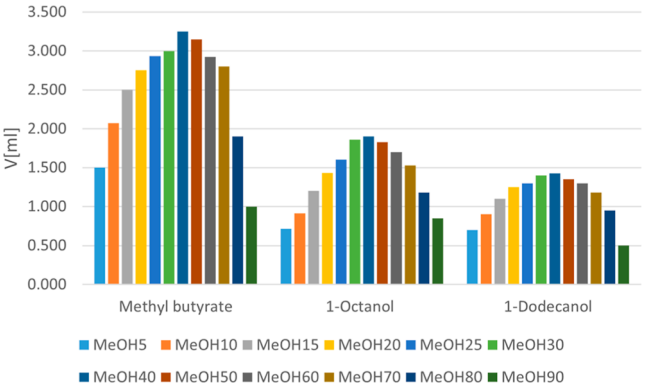

Figure 4. Volume (ml) of co-solvents added to 5 mL of MeOH-renewable diesel to achieve stable single-phase blends: colors differentiate blends with different methanol energy shares.

3.1. Performance Comparison of Oxygen-Containing Reagents

Figure 4 illustrates the amount of co-solvents added to 5 mL of mixed fuel at various methanol-renewable diesel blends, with quantities measured and reported to an accuracy of 0.0001 units. Note that, in this context, all the trends presented in Figure 4 are statistically relevant. The quantity of co-solvents required increases with the methanol content in the blend, peaking in blends containing 40% of methanol (MeOH40) for all three studied co-solvents. Beyond this point, although the methanol content continued to rise in the mixtures ranging from MeOH50 to MeOH90, the amount of co-solvent needed for a stable single-phase blend gradually decreased. Figure 5 shows the volume fraction of the co-solvents in the ternary methanol-renewable diesel (RD) co-solvent blends, based on the final total volume of the individual blends. Here, MeOHxx-Co denotes blended fuels consisting of methanol, RD, and a co-solvent at different volume ratios.

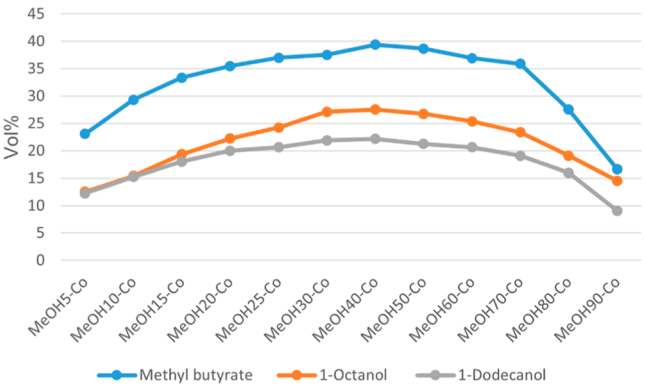

Figure 5. Volume fraction of co-solvents in ternary methanol-renewable diesel (RD)-co-solvent blends.

The nonmonotonic co-solvent demand (maximum at MeOH40) can be rationalized by the polarity contrast between the two base components and the "bridging" role of amphiphilic co-solvents. MeOH is highly polar and forms extensive hydrogen-bonded networks, whereas RD is nonpolar and

https://doi.org/10.1021/acs.jced.6c00133
J. Chem. Eng. Data 2026, 71, 2901−2913

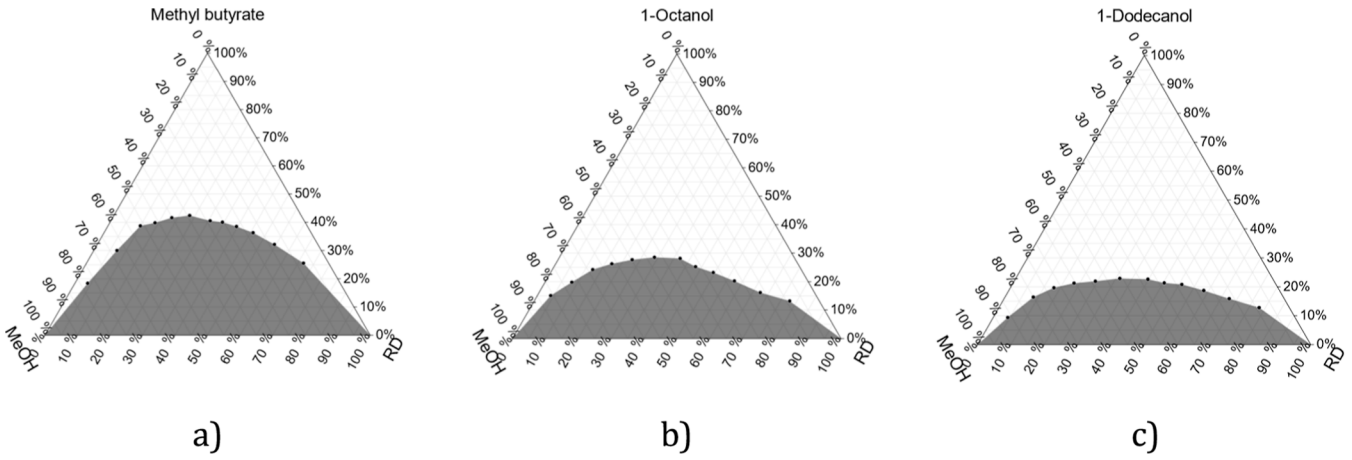

Figure 6. Phase behavior of three-component systems of methanol, renewable diesel, and co-solvents. (a) Methyl butyrate; (b) 1-octanol; and (c) 1-dodecanol at room temperature. The blend ratios of methanol, renewable diesel, and co-solvents are presented as weight fractions (wt %). The vertices correspond to 100 wt % of the respective components. Dark gray area represents two-phase liquid; white is one-phase liquid. All experimental mass-fraction data used to construct these ternary diagrams, together with the estimated uncertainties, are provided in the Supporting Information.

dominated by dispersion (van der Waals) interactions, so their direct blending leads to phase separation.[23,28,34,41] A similar peak in co-solvent requirement at intermediate alcohol/hydrocarbon blends has been reported in ternary alcohol-oil-co-solvent systems and has been attributed to the polarity contrast at those compositions.[41] Notably, although MeOH40 is defined on an energy basis, it corresponds approximately to an intermediate methanol-rich composition, which is close to the alcohol-rich mixtures (around ~7:3) reported in the literature to exhibit the maximum polarity contrast and co-solvent demand.

Co-solvents 1-octanol and 1-dodecanol, both higher alcohols with oxygen contents of 12.3% and 8.6%, respectively, were compared with methyl butyrate, which has an oxygen content of 31.4%. The results show the two higher alcohols to be more effective than methyl butyrate ester as co-solvents in forming miscible methanol-renewable diesel blends. 1-Dodecanol was the most effective in creating stable MeOH-renewable diesel blends, while methyl butyrate was the least effective. Comparison of the three oxygenated co-solvents indicates that co-solvent molecular structure, rather than oxygen content alone, governs blending performance. The higher alcohols (1-octanol and 1-dodecanol) are more effective than the ester (methyl butyrate), despite methyl butyrate's higher oxygen content. This is consistent with prior analyses showing that differences in co-solvent performance originate from how functional groups contribute to Hansen solubility parameters (HSPs) and their fractional components, especially the balance between dispersion and hydrogen-bonding contributions.[23] Hydrogen bonding and van der Waals interactions have been identified as the main driving forces for improved miscibility in alcohol−diesel systems. Hydrogen bonding dominates for short-chain alcohols, while van der Waals interactions become increasingly important for long-chain alcohols.[34] Accordingly, long-chain alcohols can bridge polar MeOH via the −OH group (hydrogen-bond donor/acceptor capability) while simultaneously interacting with paraffinic RD through the nonpolar alkyl chain (dispersion forces). In contrast, methyl butyrate lacks hydrogen-bond donor functionality and mainly acts as a hydrogen-bond acceptor through its ester group, which limits its ability to stabilize MeOH hydrogen bonding while compatibilizing RD.

Among the higher alcohols, 1-dodecanol consistently outperforms 1-octanol across the investigated blend shares. This behavior is consistent with chain-length effects reported in previous miscibility studies: a longer alkyl chain enhances dispersion interactions with diesel-like hydrocarbons while retaining −OH functionality for hydrogen-bonding interactions, thereby improving the overall amphiphilic "bridging" effectiveness.[34] Notably, both 1-octanol and 1-dodecanol demonstrated similar efficiency in enhancing the solubility of MeOH-renewable diesel blends at lower methanol concentrations (MeOH5 and MeOH10).

3.2. Effects of the Co-solvents on Phase Stability

The effect of the three co-solvents on the phase stability of MeOH-renewable diesel blends was evaluated. Figure 6 illustrates the phase behavior of the ternary system composed of methanol, renewable diesel, and the respective co-solvents at room temperature. All three co-solvents successfully maintained a stable single-phase mixture across various MeOH-renewable diesel blends.

Figures 4 and 6 show that the requirement for co-solvents to sustain a single liquid phase initially increases with increasing methanol content in the ternary system. The demand for co-solvents peaks at a methanol-to-renewable diesel blend of MeOH40, subsequently decreasing with a further increase in methanol content. This trend is consistent with previous observations reported by Jin et al.,[41] who found that in ternary systems of methanol/ethanol, soybean oil, and co-solvents, the demand for co-solvents peaked when the volume ratio of methanol/ethanol and soybean oil reached 7:3 due to the maximum polarity contrast between the components. The need for additional co-solvents decreases with a further increase of methanol/ethanol in the blends.

The white regions in Figure 6 ternary phase diagrams represent the intermiscible area of one liquid phase. The shaded regions represent the two-phase areas, indicating immiscibility and phase separation into two distinct liquid layers. Figure 6 shows that 1-dodecanol's one-phase region is larger than those of methyl butyrate and 1-octanol for the ternary system at room temperature, indicating that 1-dodecanol is the most effective co-solvent of these three. However, the white area of 1-octanol in the ternary system is not much different from that of 1-dodecanol.

https://doi.org/10.1021/acs.jced.6c00133
J. Chem. Eng. Data 2026, 71, 2901−2913

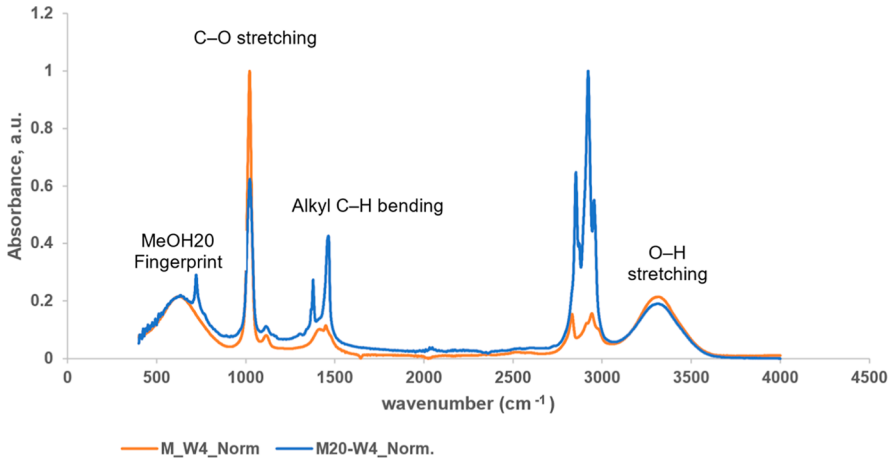

Figure 7. FTIR spectra of methanol (M) versus methanol-renewable diesel (M20) after 4 weeks storage (W4) at +20 °C.

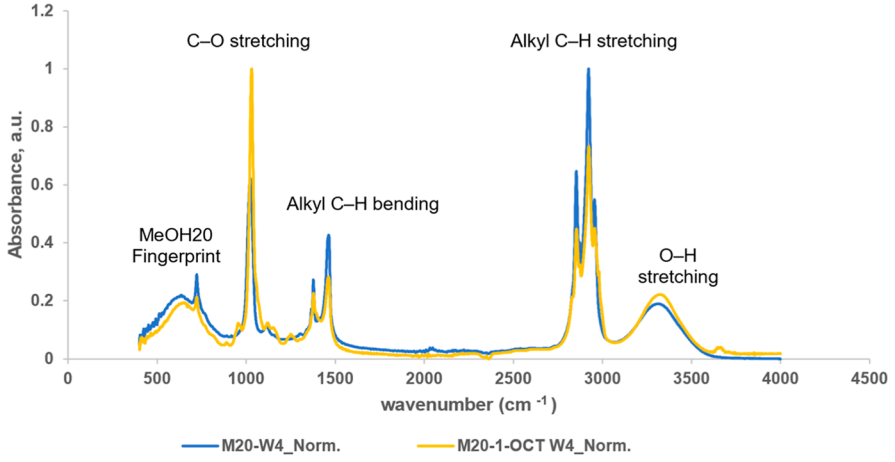

Figure 8. FTIR spectra of methanol-renewable diesel versus methanol-renewable diesel-1-octanol after 4 weeks storage (W4) at +20 °C.

3.3. FTIR Spectral Analysis for Intermolecular Interactions and Chemical Characterization

FTIR spectral analysis was used to investigate the chemical interactions and confirm the presence of specific intermolecular forces in the MeOH-renewable diesel-co-solvent blends. FTIR spectra detect differences in characteristic absorption bands associated with functional groups (e.g., O−H, C−H, C═O, and C−O), revealing interactions, hydrogen bonding, and/or polarity shifts. The methanol-renewable diesel-co-solvent blends stayed in one phase during the 4 weeks of storage. All 36 ternary blends were measured using FTIR, but only the FTIR spectra of the blend with 20% methanol, 80% renewable diesel, and co-solvent (MeOH20-RD + co-solvent) are presented here, as representative of all ternary blends. Comparisons were made between methanol and methanol-renewable diesel binary blend and between binary methanol-renewable diesel blend and ternary methanol-renewable diesel-co-solvent blends. Figures 7 and 10 present the normalized FTIR spectra.

3.3.1. Methanol vs Methanol-Renewable Diesel Binary Blend. Figure 7 compares the normalized FTIR spectra of neat methanol and the binary MeOH-renewable diesel blend after 4 weeks of storage. Neat methanol exhibits a broad and intense absorption band centered around 3345 cm^{-1} in the hydroxyl (O−H) stretching region (3200−3600 cm^{-1}), which is characteristic of strong hydrogen bonding among methanol molecules. There is a reduction in the absorption peak upon blending with renewable diesel, consistent with a lower methanol content and partial disruption of the hydrogen bonding network due to the introduced nonpolar environment. Additionally, in the alkyl C−H stretching region (2800−3000 cm^{-1}) and alkyl C−H bending region (1400−1500 cm^{-1}), the MeOH-renewable diesel blend displays stronger absorption than neat methanol, reflecting the hydrocarbon-rich structure of renewable diesel. At 2800−3000 cm^{-1}, there is dominance of C−H stretching vibrations from CH_2 and CH_3 groups in the long-chain paraffinic structure of renewable diesel in the methanol-renewable diesel blend. This contribution is largely absent in pure methanol, where the same region shows only minor contributions from sp^3 C−H stretching of the methyl group.

Pure methanol's absorption peak is notably higher in the C−O stretching band centered around 1030−1050 cm^{-1}. This absorbance decreases by approximately 40% (based on normalized peak intensities) upon blending with renewable diesel. This indicates a reduced concentration of methanol molecules contributing to C−O vibrations, while also disrupting hydrogen bond networks that reinforce methanol's characteristic absorption in this region.[36] The paraffinic hydrocarbon in renewable diesel contributes minimal absorbance in this wavenumber region, leading to an overall lower absorbance intensity for the blend. The fingerprint region (600−900 cm^{-1}) also reveals more complex spectral features in the blend,

https://doi.org/10.1021/acs.jced.6c00133
J. Chem. Eng. Data 2026, 71, 2901−2913

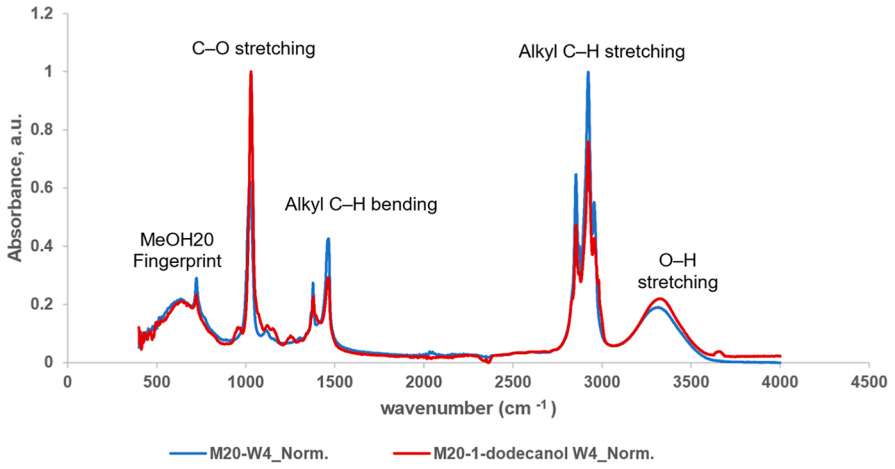

Figure 9. FTIR spectra of methanol-renewable diesel versus methanol-renewable diesel-1-dodecanol after 4 weeks storage (W4) at +20 °C.

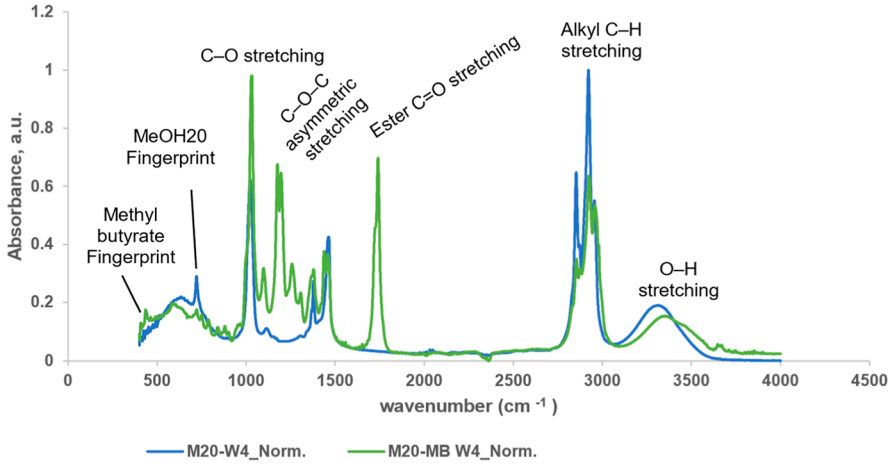

Figure 10. FTIR spectra of methanol-renewable diesel versus methanol-renewable diesel-methyl butyrate after 4 weeks storage (W4) at +20 °C.

suggesting molecular reorganization and weak dipole-induced or van der Waals interactions. Overall, the reduction in the C−O absorbance reflects dilution and weaker bulk methanol−methanol interactions.[42] Meanwhile, the emergence of paraffinic C−H mode highlights the dominance of the nonpolar paraffinic chain in the blend.[42,43] Together, these trends suggest a microheterogeneous structure in which methanol's polar domains are partially isolated by paraffinic hydrocarbons. These observations support the known immiscibility of methanol and renewable diesel, resulting from a significant mismatch in polarity and hydrogen-bonding capacity and illustrate the sensitivity of FTIR spectroscopy in resolving such intermolecular phenomena.

3.3.2. Effect of 1-Octanol and 1-Dodecanol as Co-solvent in Methanol-Renewable Diesel Ternary Blend. Figure 8 depicts the FTIR spectra of MeOH-renewable diesel blends with and without 1-octanol after 4 weeks of storage, thus evaluating the co-solvent's ability to enhance miscibility. The FTIR spectra of the methanol-renewable diesel binary blend (blue) and the methanol-renewable diesel-1-octanol ternary blend (yellow) reveal distinct changes in vibrational behavior caused by the introduction of the 1-octanol co-solvent. The C−O stretching region (1030−1050 cm^{-1}) shows higher absorbance for the ternary blend (up to 40%), indicating that the presence of 1-octanol enhances dipole moment changes in this mode.[43] This results from the additional C−O contributions for 1-octanol (same absorbance intensity in the C−O region as those in pure methanol) and altered hydrogen-bonding interactions, which reinforce this transition. In contrast, the C−H bending (1400−1500 cm^{-1}) and C−H stretching (2800−3000 cm^{-1}) regions exhibit lower absorbance in the ternary blend than in the binary blend (up to 5−10%). The observed reduction in paraffinic C−H vibrational contributions per unit concentration may be attributed to changes in molecular packing density or weakened vibrational coupling of C−H bonds upon introduction of 1-octanol.[44,45]

Interestingly, the O−H stretching region (3200−3500 cm^{-1}) shows a slight increase in absorbance for the ternary blend, implying a modified hydrogen-bonding network. While 1-octanol forms fewer hydrogen bonds than methanol, its amphiphilic structure—simultaneously forming hydrogen bonds with methanol and dispersive interaction with renewable diesel—may stabilize new hydrogen-bonding arrangements, broadening or intensifying the collective O−H vibration.[46] This structural duality makes it an effective co-solvent, consistent with solubility parameter-based predictions and visual phase stability observations. Overall, these results indicate that 1-octanol influences both polar and nonpolar contributions, while the reduction in C−H bands indicates a structural reorganization of hydrocarbon components. Meanwhile, the marginally stronger O−H band reflects altered hydrogen-bonding dynam-

https://doi.org/10.1021/acs.jced.6c00133
J. Chem. Eng. Data 2026, 71, 2901−2913

ics that may contribute to improved interfacial compatibility between methanol and diesel.[45]

Notably, the same effect observed on the FTIR spectrum for 1-octanol is evident in the FTIR spectrum for 1-dodecanol, as seen in Figure 9. In summary, the observed spectral changes, namely, the enhanced C−O absorbance, reduced C−H bending and stretching intensities, and slight increase in O−H stretching, are attributed to intermolecular interactions rather than chemical transformations. These variations reflect altered hydrogen bonding and dipole−dipole interactions introduced by 1-octanol and 1-dodecanol, which modify the molecular environment of methanol and renewable diesel, without creating new covalent bonds. The absence of new absorbance bands and retention of characteristic alcohol features indicates that the ternary blends remain a physically mixed system rather than form new species.

3.3.3. Effect of Methyl Butyrate as Co-solvent for Methanol-Renewable Diesel in Ternary Blend. In contrast to the previous two alcohol functional group co-solvents, the spectral comparison in Figure 10 reveals distinctly different behavior linked to the introduction of the ester functional group from the methyl butyrate. Most notably, the ternary blend exhibits new areas of absorption between 1000 and 1300 cm^{-1}, attributable to additional C−O stretching and C−O−C asymmetric stretching modes, characteristic of methyl butyrate.[36] This is accompanied by an increase in absorbance near the C−O stretching region (1030−1050 cm^{-1}), reflecting enhanced dipole activity and modified intermolecular interactions due to the ester functionality. Similarly, a distinct new band appears between 1500 and 2000 cm^{-1}, corresponding to the C═O stretching vibration of the ester group, which is absent in the binary blend and is a clear spectral marker of methyl butyrate incorporation. Conversely, the C−H stretching region (2800−3000 cm^{-1}) shows a decrease in absorbance intensity for the ternary blend, suggesting that the alkyl chains of methyl butyrate do not contribute strongly enough to offset the dilution of paraffinic C−H modes from renewable diesel. Similarly, the O−H stretching region (3200−3500 cm^{-1}) exhibits a reduction in intensity and a slight flattening, indicative of a disruption or weakening of the hydrogen-bonding network dominated by methanol. These decreases suggest that methyl butyrate reduces the extent of strong hydrogen-bonding interactions by introducing less polar ester groups, which interact differently with methanol compared with the alcohol−alcohol interactions in the other co-solvent cases.

Overall, the methanol-renewable diesel-methyl butyrate ternary blend spectrum reflects a shift in molecular interactions. The ester introduces new functional group vibrations while simultaneously altering existing ones through changes in polarity and hydrogen bonding. These spectral signatures indicate physical blending rather than new covalent bond formation, but they highlight how methyl butyrate modulates intermolecular forces, which influence macroscopic properties such as improved miscibility and phase stability.

4. DISCUSSION

Table 3 summarizes Hansen solubility parameters (HSPs) and fractional contributions (f_d, f_p, and f_h) for methanol, renewable diesel components, and the three selected co-solvents. Analysis of these data makes it evident that there is a significant disparity in the solubility parameters between methanol and renewable diesel components, indicating their immiscibility. This mismatch in intermolecular interactions forms the fundamental reason for phase separation in binary methanol-renewable diesel blends. The polarity gap between methanol (high f_h) and renewable diesel (zero f_h) is bridged by co-solvents that combine dispersion forces with hydrogen-bonding capability.

Methanol exhibits $f_d = 0.30$, $f_p = 0.25$, and $f_h = 0.45$, indicating a dominant hydrogen-bonding contribution (45%). Renewable diesel components such as hexadecane and octadecane are purely dispersion-driven ($f_d = 1.0$, $f_p = 0$, and $f_h = 0$), which accounts for their immiscibility with methanol.

Methanol's strong polar and hydrogen-bonding forces are absent in diesel fuels,[23,40,47] resulting in a pronounced imbalance in intermolecular forces among methanol−methanol, methanol-renewable diesel, and renewable diesel-renewable diesel molecules. The alcohols (1-octanol and 1-dodecanol) possess dispersion solubility parameters similar to those of renewable diesel components and moderate polar and hydrogen-bonding parameters. Among the co-solvents, 1-octanol ($f_d = 0.49$, $f_p = 0.15$, and $f_h = 0.36$) demonstrates amphiphilic behavior, balancing dispersion, and hydrogen bonding interactions to interact with both methanol and diesel. 1-Dodecanol ($f_d = 0.54$, $f_p = 0.14$, and $f_h = 0.32$) shows an even higher dispersion share, due to its longer alkyl chain, reducing polarity, and presenting good hydrogen bonding capability, making it the most effective co-solvent in this study. Literature did not provide values for methyl butyrate's fractional contributions, which limits quantitative comparison and highlights a methodological constraint in interpreting ester in MeOH-RD interactions.

The oxygen-containing functional groups in alcohols and esters are hydroxyl (−OH) and ester linkage (−COO−), respectively. These groups function as hydrophilic units, with their water affinity varying based on the number of hydrogen-bond donors and acceptors they possess.[23] As summarized in the study by Gao et al.,[23] the hydroxyl group (−OH) exhibits both one hydrogen bond donor and one acceptor. In contrast, methyl butyrate contains an ester functional group that can act as a hydrogen-bond acceptor but lacks hydrogen-bond donor capability. These differences highlight that alcohol-based co-solvents, such as 1-octanol and 1-dodecanol, are more capable of establishing hydrogen-bonding interactions with methanol, whereas methyl butyrate relies primarily on polarity-based interactions. Such variations in donor/acceptor balance and corresponding HSP contributions are expected to affect the miscibility and phase stability of the blends. These results indicate that co-solvent effectiveness is governed primarily by the balance between hydrogen bonding and dispersion interactions, rather than oxygen content alone.

4.1. Evidence of Physical Interactions without New Covalent Bond Formation and Spectroscopic Validation of Co-solvent Efficiency

Across all FTIR spectra, including the one binary and three ternary blends, the spectral changes are consistent with physical interactions rather than the formation of new covalent bonds. In the 1-octanol and 1-dodecanol blends, the increased C−O absorbance and broadened O−H stretching region (3200−3500 cm^{-1}) reflect stronger hydrogen bonding and enhanced C−O vibrational coupling. Their reduction in C−H bending and stretching intensities indicates dilution of paraffinic modes. In contrast, the methyl butyrate blends introduce new ester-specific peaks, C−O−C and enhanced C−O modes (1000−1300 cm^{-1}) and a distinct C═O band (1500−2000 cm^{-1}) but also show decreased C−H stretching and flattened O−H absorbance, suggesting disruption of methanol's hydrogen-bonding network.

https://doi.org/10.1021/acs.jced.6c00133
J. Chem. Eng. Data 2026, 71, 2901−2913

Crucially, none of the blends exhibits spectral signatures of chemical reaction.

These observations confirm that the blends are physically mixed systems, with their spectral behavior governed by noncovalent interactions, such as hydrogen bonding, dipole−dipole interaction, and van der Waals forces, rather than by chemical transformation. Dispersion interactions become stronger as the alkyl chain length increases, due to increased molecular size and polarizability, leading to improved compatibility with renewable diesel.[48−50] These effects, observed through FTIR and fitting into the HSP theory, show that the longer-chain alcohol (1-dodecanol) has a greater influence and is a more effective co-solvent than the shorter-chain alcohol (1-octanol).

Co-solvents 1-octanol and 1-dodecanol have the same dispersion solubility value 16, although they have different polar and hydrogen bonding solubilities, as shown in Table 3. This characteristic enhances the ability of higher alcohols, compared with methanol, to blend in a stable way with renewable diesel. Figure 5 shows that smaller amounts of the longer alkyl-chain alcohol are needed to create stable methanol-renewable diesel blends. This is consistent with the findings of Liu et al.,[47] showing that alcohols with higher carbon numbers provide a better intersoluble capacity. Importantly, these findings are in accordance with the spectroscopic analysis. FTIR demonstrated that the longer-chain alcohols strengthen hydrogen bonding and dispersion interactions without forming new covalent bonds. Alcohol chain length appears to be a key factor in phase stability: longer alcohols provide stronger noncovalent interactions and more favorable solubility parameters, thereby stabilizing methanol-renewable diesel blends more effectively than short-chain alcohols.

The comparative FTIR analyses clearly distinguish the mechanistic differences among the tested co-solvents. The FTIR features summarized in Table 4 further support these observations. Methanol and renewable diesel possess significantly mismatched Hansen solubility parameter (HSP) values, particularly in the hydrogen-bonding and polar-interacting components. 1-Dodecanol, with dual polarity and the ability to form hydrogen bonds, effectively promotes molecular−level interactions, just ahead of 1-octanol, validating their selection as a co-solvent based on HSP values (1-dodecanol: δ_d = 16.0; δ_p = 4; δ_h = 9.3; and 1-octanol: δ_d = 16.0; δ_p = 5; δ_h = 11.9). This supports the broader finding that a co-solvent with suitable amphiphilic properties can significantly enhance the miscibility of otherwise incompatible fuel components.

4.2. Co-solvent Selection, Limitations, and Outlook

The combined phase behavior, HSP analysis, and FTIR results indicate that effective co-solvents require amphiphilic characteristics, enabling them to balance dispersion and hydrogen-bonding interactions. For the investigated systems, co-solvents with dispersion solubility parameter δ_d = 16 and fractional dispersion contributions f_d = 0.49−0.54, such as 1-octanol and 1-dodecanol, were found to be effective in forming stable methanol-renewable diesel blends. This observation is consistent with the FTIR analysis, which shows that these co-solvents enhance intermolecular interactions without inducing chemical reactions. However, these values should be interpreted as system-specific guidelines rather than universal criteria, as the analysis is limited to a small number of co-solvents, and HSP data for methyl butyrate is incomplete.

Table 4. Summary of FTIR Spectral Features of Binary and Ternary MeOH-Renewable Diesel (RD) Blends with Different Co-solvents

blend type	spectral regions (cm^{-1})	key interpretation
MeOH-RD (binary)	1000−1100 (C−O stretch); 1300−1500 (C−H bend); 2800−3000 (C−H stretch); 3200−3500 (O−H stretch)	weakened C−O and O−H stretch absorbance from methanol as hydrogen-bonding networks break down in a nonpolar environment; prominent C−H stretch of alkanes, indicative of paraffinic content
MeOH-RD + 1-octanol (ternary)	1000−1100 (C−O stretch); 1300−1500 (C−H bend); 2800−3000 (C−H stretch); 3200−3500 (O−H stretch)	enhanced C−O absorbance due to stronger hydrocarbon bonding and C−O vibrational coupling; reduced C−H bending/stretching; slightly higher and broadened O−H region; better hydrogen-bonding network from co-solvent amphiphilic contribution disrupting tightly packed alkyl chain; can act both as a hydrogen donor and acceptor, enhancing the hydrogen-bonding network
MeOH-RD + 1-dodecanol (ternary)	1000−1100 (C−O stretch); 1300−1500 (C−H bend); 2800−3000 (C−H stretch); 3200−3500 (O−H stretch)	enhanced C−O absorbance due to stronger hydrocarbon bonding and C−O vibrational coupling; reduced C−H bending/stretching; slightly higher and broadened O−H region due to enhanced hydrogen-bonding network (can operate as both hydrogen donor and acceptor); strongest co-solvent effect due to stronger amphiphilic contribution resulting from longer alkyl chain from alcohol
MeOH-RD + methyl butyrate (ternary)	1000−1300 (C−O & C−O−C stretch); 1500−2000 (C=O stretch); 2800−3000 (C−H stretch); 3200−3500 (O−H stretch)	observable ester-specific peaks (C−O−C and C=O); increased C−O region; decreased C−H stretching and flattened O−H stretching, indicating disrupted and weaker hydrogen bonding (as it lacks a hydrogen bond donor but can only act as acceptor); comparatively lowest blending effectiveness

https://doi.org/10.1021/acs.jced.6c00133
J. Chem. Eng. Data 2026, 71, 2901−2913

This study has several limitations. The experiments were conducted at room temperature, and the temperature-dependent phase behavior was not investigated. Phase stability assessment relied on visual observation and FTIR analysis after storage without systematic long-term stability testing under varying conditions. In addition, only a limited number of co-solvents were studied, and the HSP comparison was constrained by incomplete parameter data for methyl butyrate. Furthermore, this work focused solely on miscibility and intermolecular interactions: it did not evaluate fuel properties relevant to engine applications, such as viscosity, ignition quality, spray behavior, combustion performance, and emissions. However, the fuel properties of the studied blends have already been analyzed in a previous study by Wang-Alho et al.,[20] and the blends of methanol, renewable diesel, and 1-octanol were validated with engine experiments.[51] The fuel blends as drop-in resulted in similar combustion and emission behavior with diesel, with similar or even better brake thermal efficiency, especially at low load and providing lower CO_2 emissions.

Future work should extend co-solvent screening to a broader range of oxygenated compounds with well-characterized HSP values. Temperature-dependent phase behavior and long-term stability were systematically studied.

5. CONCLUSIONS

The present work investigated the performance of different oxygen-containing co-solvents in improving the solubility of methanol in renewable diesel. The aim was to find a suitable co-solvent for methanol in renewable diesel blends. Molecular structure and intermolecular forces were also analyzed. Key conclusions can be summarized as follows.

- Immiscibility between methanol and renewable diesel is due to differences in their solubility parameters, especially polar force and hydrogen bonding force parameters.
- FTIR analysis revealed that co-solvent choice strongly influences methanol-renewable diesel miscibility. In the binary system, methanol's hydrogen-bonding network is disrupted, while renewable diesel's paraffinic character dominates. The co-solvent 1-octanol improved C−O coupling and stabilized hydrogen bonding via its amphiphilic nature, whereas 1-dodecanol, with a longer alkyl chain, provided the strongest enhancement. Methyl butyrate, lacking hydrogen-bond donor capability, weakens hydrogen bonding but shows the poorest blending performance.
- FTIR analysis revealed that none of the studied co-solvents produced covalent bonds in the chemical structure of methanol-renewable diesel blends.
- Of the investigated co-solvents, 1-dodecanol exhibited the best performance in terms of solubility. Less 1-dodecanol was needed to prepare stable methanol-renewable diesel blends. 1-Octanol also showed good performance as a co-solvent. The co-solvents 1-octanol and 1-dodecanol showed the same performance with MeOH5 and MeOH10 blends.
- Oxygen-containing co-solvents with different functional groups and HSP values can balance intermolecular forces, enhancing methanol-renewable diesel miscibility. For 1-octanol and 1-dodecanol, the fractional contributions for f_d were 0.49 and 0.54, respectively. The dispersion solubility parameter δ_d = 16 can be a reference for choosing a suitable co-solvent to prepare methanol-renewable blends.

The findings of this study provide new insights into the molecular mechanisms governing compatibility in methanol-renewable diesel mixtures. The study demonstrates that miscibility and phase stability are controlled primarily by intermolecular interactions rather than chemical modification. The results also offer a useful reference for addressing miscibility challenges in other oxygenate-hydrocarbon systems, which is important for accelerating the wider adoption of methanol as a practical alternative fuel. Furthermore, the demonstrated ability of higher alcohol co-solvents to form stable, single-phase methanol-renewable diesel blends presents a promising pathway toward single-fuel injection operation, simplifying fuel-system design compared with dual-fuel pilot-ignited concepts.

■ ASSOCIATED CONTENT

Data Availability Statement

The experimental FTIR data sets generated and analyzed during the current study are available from the corresponding author upon reasonable request.

Supporting Information

The Supporting Information is available free of charge at https://pubs.acs.org/doi/10.1021/acs.jced.6c00133.

Complete ternary mass-fraction composition data; MeOH, renewable diesel, and co-solvent, together with estimated uncertainties in co-solvent mass fraction based on pipet accuracy (PDF)

■ AUTHOR INFORMATION

Corresponding Authors

Huaying Wang-Alho − *School of Technology and Innovations, Energy Technology, University of Vaasa, Vaasa 65200, Finland*; orcid.org/0009-0000-0777-2001; Email: huaying.wang-alho@uwasa.fi

Fatimoh Balogun − *School of Technology and Innovations, Energy Technology, University of Vaasa, Vaasa 65200, Finland*; orcid.org/0009-0001-2425-0982; Email: fatimoh.balogun@uwasa.fi

Authors

Katriina Sirviö − *School of Technology and Innovations, Energy Technology, University of Vaasa, Vaasa 65200, Finland*

Carolin Nuortila − *School of Technology and Innovations, Energy Technology, University of Vaasa, Vaasa 65200, Finland*

David Thomas − *School of Technology and Innovations, Energy Technology, University of Vaasa, Vaasa 65200, Finland*

Maciej Mikulski − *School of Technology and Innovations, Energy Technology, University of Vaasa, Vaasa 65200, Finland*

Seppo Niemi − *School of Technology and Innovations, Energy Technology, University of Vaasa, Vaasa 65200, Finland*

Complete contact information is available at: https://pubs.acs.org/10.1021/acs.jced.6c00133

Author Contributions

Conceptualization: H.W.-A. and K.S.; methodology: H.W.-A., K.S., and F.B.; investigation: H.W.-A., K.S., and F.B.; resources: K.S., M.M., and S.N.; data curation: H.W.-A. and F.B.; data

https://doi.org/10.1021/acs.jced.6c00133
J. Chem. Eng. Data 2026, 71, 2901−2913

analysis and interpretation: H.W.-A., F.B., K.S., D.T., and C.N.; writing—original draft preparation: H.W.-A. and F.B.; writing—review and editing: H.W.-A., F.B., K.S., D.T., and C.N.; visualization: H.W.-A. and F.B.; supervision: K.S., M.M., and S.N.; project administration: M.M.; funding acquisition: K.S., M.M., and S.N. All authors have read and agreed to the published version of the manuscript.

Funding

The work was conducted in the framework of the Flexible Clean Propulsion Technologies project with financial support from Business Finland (ref 1310/31/2023).

Notes

The authors declare no competing financial interest.

■ ACKNOWLEDGMENTS

The authors wish to thank Neste for providing the renewable diesel for this research.

■ REFERENCES

(1) Jin, C.; Sun, T.; Yin, Z.; Han, W.; Zhang, C.; Geng, Z.; Li, X.; Dong, J.; Xu, T.; Ji, J.; Wang, G.; Liu, H. Preparation and Properties Analysis of Ethanol/Furan-Derivative/Diesel Alternative Microemulsion Fuel. *Fuel Process. Technol.* **2022**, *235*, 107383.

(2) Kalair, A.; Abas, N.; Saleem, M. S.; Kalair, A. R.; Khan, N. Role of Energy Storage Systems in Energy Transition from Fossil Fuels to Renewables. *Energy Storage* **2021**, *3* (1), No. e135.

(3) Blondeel, M.; Bradshaw, M. J.; Bridge, G.; Kuzemko, C. The Geopolitics of Energy System Transformation: A Review. *Geogr. Compass* **2021**, *15* (7), No. e12580.

(4) Dimitriadis, A.; Natsios, I.; Dimaratos, A.; Katsaounis, D.; Samaras, Z.; Bezergianni, S.; Lehto, K. Evaluation of a Hydrotreated Vegetable Oil (HVO) and Effects on Emissions of a Passenger Car Diesel Engine. *Front. Mech. Eng.* **2018**, *4*, 7.

(5) Leijon, J.; Boström, C. Charging Electric Vehicles Today and in the Future. *World Electric Vehicle Journal* **2022**, *13*, 139.

(6) Yue, Z.; Liu, H. Advanced Research on Internal Combustion Engines and Engine Fuels. In *Energies*; Multidisciplinary Digital Publishing Institute, 2023.

(7) Mantoam, E. J.; Romanelli, T. L.; Gimenez, L. M. Energy Demand and Greenhouse Gases Emissions in the Life Cycle of Tractors. *Biosyst. Eng.* **2016**, *151*, 158−170.

(8) Jin, C.; Liu, X.; Sun, T.; Dankwa Ampah, J.; Geng, Z.; Ikram, M.; Ji, J.; Wang, G.; Liu, H. Preparation of Ethanol and Palm Oil/Palm Kernel Oil Alternative Biofuels Based on Property Improvement and Particle Size Analysis. *Fuel* **2021**, *305*, 121569.

(9) 2023 IMO STRATEGY ON REDUCTION OF GHG EMISSIONS FROM SHIPS.

(10) Wissner, N.; Healy, S.; Cames, M.; Sutter, J. Methanol as a Marine Fuel, 2023. https://safety4sea.com/wp-content/uploads/2023/03/NABU-methanol-study-2023_03.pdf (accessed Oct, 20 2025).

(11) Salehi, R.; Chaiprapat, S. Conversion of Biogas from Anaerobic Digestion to Single Cell Protein and Bio-Methanol: Mechanism, Microorganisms and Key Factors-A Review. *Environ. Eng. Res.* **2021**, *27*..

(12) Ming, L. Methanol as a Marine Fuel-Availability and Pre-Trial Considerations; 2020. https://www.ntu.edu.sg/docs/librariesprovider79/publication/mesd-webinar-2020-methanol-as-a-marine-fuel.pdf (accessed Oct, 20 2025).

(13) Ciniviz, M.; Köse, H.; Canli, E.; Solmaz, O. An Experimental Investigation on Effects of Methanol Blended Diesel Fuels to Engine Performance and Emissions of a Diesel Engine. *Sci. Res. Essays* **2011**, *6* (15), 3189−3199.

(14) Duan, Q.; Yin, X.; Wang, X.; Kou, H.; Zeng, K. Experimental Study of Knock Combustion and Direct Injection on Knock Suppression in a High Compression Ratio Methanol Engine. *Fuel* **2022**, *311*, 122505.

(15) Hunicz, J.; Mikulski, M.; Shukla, P. C.; Gęca, M. S. Partially Premixed Combustion of Hydrotreated Vegetable Oil in a Diesel Engine: Sensitivity to Boost and Exhaust Gas Recirculation. *Fuel* **2022**, *307*, 121910.

(16) Niemi, S.; Vauhkonen, V.; Mannonen, S.; Ovaska, T.; Nilsson, O.; Sirviö, K.; Heikkilä, S.; Kiijärvi, J. Effects of Wood-Based Renewable Diesel Fuel Blends on the Performance and Emissions of a Non-Road Diesel Engine. *Fuel* **2016**, *186*, 1−10.

(17) Spoof-Tuomi, K.; Vauhkonen, V.; Niemi, S.; Ovaska, T.; Lehtonen, V.; Heikkilä, S.; Nilsson, O. Effects of Crude Tall Oil Based Renewable Diesel on the Performance and Emissions of a Non-Road Diesel Engine. In *SAE Technical Papers; SAE International*; SAE Internationa, 2021..

(18) Hunicz, J.; Matijošius, J.; Rimkus, A.; Kilikevičius, A.; Kordos, P.; Mikulski, M. Efficient Hydrotreated Vegetable Oil Combustion under Partially Premixed Conditions with Heavy Exhaust Gas Recirculation. *Fuel* **2020**, *268*, 117350.

(19) Ammar, N. R. An Environmental and Economic Analysis of Methanol Fuel for a Cellular Container Ship. *Transp. Res. D Transp. Environ.* **2019**, *69*, 66−76.

(20) Wang-Alho, H.; Sirviö, K.; Balogun, F.; Kaivosoja, J.; Nuortila, C.; Mikulski, M.; Niemi, S. Properties of Chemically Stabilized Methanol−HVO Blends. *Energies* **2024**, *17* (15), 3724.

(21) Jin, C.; Zhang, X.; Han, W.; Geng, Z.; Tessa Margaret Thomas, M.; Dankwa Jeffrey, A.; Wang, G.; Ji, J.; Liu, H. Macro and Micro Solubility between Low-Carbon Alcohols and Rapeseed Oil Using Different Co-Solvents. *Fuel* **2020**, *270*, 117511.

(22) Pandey, A.; Gangil, S.; Vyas, S.; Gaur, A. International Journal of Emerging Technology and Advanced Engineering Ethanol-Diesel and Bio-Diesel Blend as Substitute Fuel to CI Engines A Comprehensive Review; 2008; Vol. 9001. www.ijetae.com (accessed Oct, 10 2025).

(23) Gao, Z.; Wu, S.; Luo, J.; Zhang, B.; Zhang, H.; Xiao, R. Optimize the Co-Solvent for Methanol in Diesel with Group of Oxygen-Containing Reagents: Molecular Structure and Intermolecular Forces Analysis. *Fuel Process. Technol.* **2021**, *222*, 106980.

(24) Nils-Olof, N.; Päivi, A.; Niemi, S.; Paanu, T.; Polytechnic, T.; Berg, R.; Konsult, B. ALCOHOLS/ETHERS AS OXYGENATES IN DIESEL FUEL: PROPERTIES OF BLENDED FUELS AND EVALUATION OF PRACTICAL EXPERIENCES IEA ADVANCED MOTOR FUELS ANNEX XXVI FINAL REPORT, 2005. https://www.iea-amf.org/app/webroot/files/file/Annex%20Reports/AMF_Annex_26.pdf (accessed Oct, 10 2025)..

(25) Wang, X.; Cheung, C. S.; Di, Y.; Huang, Z. Diesel Engine Gaseous and Particle Emissions Fueled with Diesel-Oxygenate Blends. *Fuel* **2012**, *94*, 317−323.

(26) Ren, Y.; Huang, Z.; Miao, H.; Di, Y.; Jiang, D.; Zeng, K.; Liu, B.; Wang, X. Combustion and Emissions of a DI Diesel Engine Fuelled with Diesel-Oxygenate Blends. *Fuel* **2008**, *87* (12), 2691−2697.

(27) Liu, H.; Wang, X.; Wu, Y.; Zhang, X.; Jin, C.; Zheng, Z. Effect of Diesel/PODE/Ethanol Blends on Combustion and Emissions of a Heavy Duty Diesel Engine. *Fuel* **2019**, *257*, 116064.

(28) El-Seesy, A. I.; El-Zoheiry, R. M.; Fouad, A. K.; Hussien, A. M.; Elshabrawy, S. O. M.; He, Z.; Nasser, A. Impacts of Octanol and Decanol Addition on the Solubility of Methanol/Hydrous Methanol/Diesel/Biodiesel/Jet A-1 Fuel Ternary Mixtures. *RSC Adv.* **2021**, *11* (30), 18213−18224.

(29) Verhelst, S.; Turner, J. W.; Sileghem, L.; Vancoillie, J. Methanol as a Fuel for Internal Combustion Engines. *Prog. Energy Combust. Sci.* **2019**, *70*, 43−88.

(30) Waluyo, B.; Setiyo, M.; Saifudin; Wardana, I. N. G. The Role of Ethanol as a Cosolvent for Isooctane-Methanol Blend. *Fuel* **2020**, *262*, 116465.

(31) Waluyo, B.; Setiyo, M.; Saifudin; Wardana, I. N. G. Fuel Performance for Stable Homogeneous Gasoline-Methanol-Ethanol Blends. *Fuel* **2021**, *294*, 120565.

(32) Türck, J.; Singer, A.; Lichtinger, A.; Almaddad, M.; Türck, R.; Jakob, M.; Garbe, T.; Ruck, W.; Krahl, J. Solketal as a Renewable Fuel

Component in Ternary Blends with Biodiesel and Diesel Fuel or HVO and the Impact on Physical and Chemical Properties. *Fuel* **2022**, *310*, 122463.
(33) Neste Renewable Diesel Handbook, 2020. https://static1.squarespace.com/static/6155b5bdada6ea1708c2c74d/t/64c9f97e9ecd6242f77ffe04/1690958493039/2016-05+Neste+Renewable+Diesel+Handbook.pdf (accessed Jan, 09, 2026).
(34) Li, X.; Hou, L.; Chai, C.; He, S.; Huang, Y. A New Molecular Insight in Effects of Alcohol Co-Solvents on Miscibility of Anhydrous Ethanol/Diesel Blends. *J. Energy Resour. Technol.* **2023**, *145* (4), 041303.
(35) Jin, C.; Sun, T.; Ampah, J. D.; Liu, X.; Geng, Z.; Afrane, S.; Yusuf, A. A.; Liu, H. Comparative Study on Synthetic and Biological Surfactants' Role in Phase Behavior and Fuel Properties of Marine Heavy Fuel Oil-Low Carbon Alcohol Blends under Different Temperatures. *Renew. Energy* **2022**, *195*, 841−852.
(36) Balogun, F.; Wang-Alho, H.; Sirviö, K.; Mikulski, M. FTIR Analysis for Determining Stability of Methanol−HVO Blends for Non-Road Engine Application. *Energies* **2024**, *17* (16), 3921.
(37) Lampinen, A. Uusiutuvan Liikenne-Energian Tiekartta. PhD Thesis, 2009..
(38) Wang-Alho, H.; Sirviö, K.; Hissa, M.; Mikulski, M.; Niemi, S. Methanol-HVO Blends for Efficient Low-Temperature Combustion: Analytical Research on Fuel Properties. *Agronomy Research* **2023**, *21* (2), 994−1005.
(39) *National Library of Medicine*; National Center for Biotechnology Information: USA 2025..
(40) Charles, M. H. *Hansen Solubility Parameters A User's Handbook*, 2nd ed.; CRC Press, 2007.
(41) Jin, C.; Zhang, X.; Geng, Z.; Pang, X.; Wang, X.; Ji, J.; Wang, G.; Liu, H. Effects of Various Co-Solvents on the Solubility between Blends of Soybean Oil with Either Methanol or Ethanol. *Fuel* **2019**, *244*, 461−471.
(42) Böhm, J.; Bopp, P. A.; Soetens, J. C. Water-Methanol Mixtures: Investigations of Their Peculiar Mixing Properties by Means of Molecular Dynamics Simulations. *J. Mol. Liq.* **2025**, *425*, 127194.
(43) Tammer, M. G. Sokrates: Infrared and Raman Characteristic Group Frequencies: Tables and Charts. *Colloid Polym. Sci.* **2004**, *283* (2), 235.
(44) Wang, Z.; Dan, G.; Zhang, R.; Ma, L.; Lin, K. Coupling and Decoupling CH Stretching Vibration of Methylene and Methine in Serine Conformers. *Spectrochim. Acta A Mol. Biomol. Spectrosc.* **2023**, *285*, 121829.
(45) Palombo, F.; Tassaing, T.; Danten, Y.; Besnard, M. Hydrogen Bonding in Liquid and Supercritical 1-Octanol and 2-Octanol Assessed by near and Midinfrared Spectroscopy. *J. Chem. Phys.* **2006**, *125* (9), 094503.
(46) Fatty Alcohols (Octanol and Decanol) Crops, 2016. https://www.ams.usda.gov/sites/default/files/media/FattyAlcohols020217.pdf (accessed Nov, 05, 2025).
(47) Liu, H.; Hu, B.; Jin, C. Effects of Different Alcohols Additives on Solubility of Hydrous Ethanol/Diesel Fuel Blends. *Fuel* **2016**, *184*, 440−448.
(48) Nochebuena, J.; Piquemal, J. P.; Liu, S.; Cisneros, G. A. Cooperativity and Frustration Effects (or Lack Thereof) in Polarizable and Non-Polarizable Force Fields. *J. Chem. Theory Comput.* **2023**, *19* (21), 7715−7730.
(49) Assaf, K. I.; Nau, W. M. Dispersion Interactions in Condensed Phases and inside Molecular Containers. *Acc. Chem. Res.* **2023**, *56* (23), 3451−3461.
(50) Danovich, D.; Tkatchenko, A.; Alvarez, S.; Shaik, S. A Gravitational-like Relationship of Dispersion Interactions Is Exhibited by 40 Pairs of Molecules and Noble Gas Atoms. *J. Am. Chem. Soc.* **2024**, *146* (45), 31198−31204.
(51) Wang-Alho, H.; Pohjolainen, O.; Tajwar, M. R.; Ovaska, T.; Belgiorno, G.; Sirviö, K.; Hunicz, J.; Mikulski, M. Performance and Emissions of Stabilized Methanol-Renewable Diesel Blends in a Tier 4F Non-road Diesel Engine. *Proceedings of the ASME 2026. September 14−16*; American Society of Mechanical Engineers, 2026, Detroit, MI, USA. In press..

https://doi.org/10.1021/acs.jced.6c00133
J. Chem. Eng. Data 2026, 71, 2901−2913